Transferable Potentials for Phase Equilibria. 8. United-Atom Description for Thiols, Sulfides, Disulfides, and Thiophene

ARTICLE *in* THE JOURNAL OF PHYSICAL CHEMISTRY B · JANUARY 2006

Impact Factor: 3.3 · DOI: 10.1021/jp0549125 · Source: PubMed

THE JOURNAL OF PHYSICAL CHEMISTRY B

Article

Transferable Potentials for Phase Equilibria. 8. United-Atom Description for Thiols, Sulfides, Disulfides, and Thiophene

Nusrat Lubna, Ganesh Kamath, Jeffrey J. Potoff, Neeraj Rai, and J. Ilja Siepmann

J. Phys. Chem. B, **2005**, 109 (50), 24100-24107 • DOI: 10.1021/jp0549125

Transferable Potentials for Phase Equilibria. 8. United-Atom Description for Thiols, Sulfides, Disulfides, and Thiophene

Nusrat Lubna,[†] Ganesh Kamath,[†] Jeffrey J. Potoff,*[,†] Neeraj Rai,[‡] and J. Ilja Siepmann[‡]

Department of Chemical Engineering and Materials Science, Wayne State University, 5050 Anthony Wayne Drive, Detroit, Michigan 48202, and Departments of Chemistry and of Chemical Engineering and Materials Science, University of Minnesota, 207 Pleasant Street Southeast, Minneapolis, Minnesota 55455-0431

Received: August 30, 2005; In Final Form: October 24, 2005

An extension of the transferable potentials for phase equilibria united-atom (TraPPE-UA) force field to thiol, sulfide, and disulfide functionalities and thiophene is presented. In the TraPPE-UA force field, nonbonded interactions are governed by a Lennard−Jones plus fixed point charge functional form. Partial charges are determined through a CHELPG analysis of electrostatic potential energy surfaces derived from ab initio calculations at the HF/6-31g+(d,p) level. The Lennard−Jones well depth and size parameters for four new interaction sites, S (thiols), S(sulfides), S(disulfides), and S(thiophene), were determined by fitting simulation data to pure-component vapor-equilibrium data for methanethiol, dimethyl sulfide, dimethyl disulfide, and thiophene, respectively. Configurational-bias Monte Carlo simulations in the grand canonical ensemble combined with histogram-reweighting methods were used to calculate the vapor−liquid coexistence curves for methanethiol, ethanethiol, 2-methyl-1-propanethiol, 2-methyl-2-propanethiol, 2-butanethiol, pentanethiol, octanethiol, dimethyl sulfide, diethyl sulfide, ethylmethyl sulfide, dimethyl disulfide, diethyl disulfide, and thiophene. Excellent agreement with experiment is achieved, with unsigned errors of less than 1% for saturated liquid densities and less than 3% for critical temperatures. The normal boiling points were predicted to within 1% of experiment in most cases, although for certain molecules (pentanethiol) deviations as large as 5% were found. Additional calculations were performed to determine the pressure−composition behavior of ethanethiol+*n*-butane at 373.15 K and the temperature−composition behavior of 1-propanethiol+*n*-hexane at 1.01 bar. In each case, a good reproduction of experimental vapor−liquid equilibrium separation factors is achieved; both of the coexistence curves are somewhat shifted because of overprediction of the pure-component vapor pressures.

1. Introduction

There is considerable interest in the physical properties of sulfur-containing compounds, particularly in the petroleum industry. Increasingly strict regulations designed to reduce emissions from internal combustion engines and the need to process feedstocks with greater levels of sulfur are forcing refineries to rethink their refinement strategies. Despite the need for such data, only limited vapor−liquid equilibrium data are available in the literature. The most comprehensive of these is a study by Denyer et al. who investigated the formation of azeotropes between 7 low molecular weight thiols and 28 different hydrocarbons.[1] In addition, temperature composition behavior is presented for binary mixtures of propanethiol with *n*-hexane, methylcyclopentane, and 2-methylpentane. Experimental pressure−composition data are available for the mixtures methanethiol+*n*-hexane[2] and ethanethiol+*n*-butane,[3] while dew and bubble points have been determined for binary mixtures of low molecular weight thiols with *n*-hexane, *n*-decane, toluene, or water for mole fractions of thiol < 0.2.[4] Finally, a review discussing experimental measurements of the critical properties of sulfur-containing compounds has been published recently.[5]

Equation-of-state models utilizing complex mixing rules for the excess Gibbs, G^E, and Helmholtz energies, A^E, have been proposed for modeling the vapor−liquid equilibria (VLE) of thiol/hydrocarbon mixtures.[6] Overall, such a methodology was shown to provide a very good reproduction of mixture phase behavior. However, the use of an equation of state requires, at the bare minimum, knowledge of the critical temperature and pressure for each of the components, quantities that are not always available. Molecular simulation provides an alternative route to the calculation of VLE, with improved predictive capabilities when compared to equation-of-state modeling.

The accuracy of molecular simulation is linked directly to the intermolecular potentials, also referred to as "force fields," used in the calculations. Although a large number of force fields may be found in the literature,[7−11] only a handful have been parametrized specifically for calculation of vapor−liquid equilibria. After an initial proliferation of united-atom force fields for *n*-alkanes based on exponential-6[12] and Lennard−Jones[13−15] functional forms, the generation of high-accuracy force fields for polar molecules has proven to be more difficult. Only recently have force fields appeared in the literature for VLE predictions of alcohols,[16,17] carboxylic acids,[18] ketones,[19,20] thiols, and sulfides.[21]

Starting with a generalized force field for alkanes,[13,22] it has been the ongoing goal of our research groups to create a transferable and computationally efficient force field for general use in simulations. Known as TraPPE (transferable potentials

* To whom correspondence should be addressed. E-mail: jpotoff@chem1.eng.wayne.edu. Fax: 313-577-3810. Phone: 313-577-9357.
[†] Wayne State University.
[‡] University of Minnesota.

10.1021/jp0549125 CCC: $30.25
Published on Web 11/25/2005

TABLE 1: TraPPE-UA Force Field Parameters for Nonbonded Interactions

site	molecule	ϵ/k_b (K)	σ (Å)	q(e)
$CH_3(sp^3)$	thiol/sulfide/disulfide	98	3.75	+0.171[a]/0.15[b]/0.177[c]
$CH_2(sp^3)$	thiol/sulfide/disulfide	46	3.95	+0.171[a]/0.15[b]/0.177[c]
$CH_3(sp^3)$	all other	98	3.75	0.0
$CH_2(sp^3)$	all other	46	3.95	0.0
$CH(sp^3)$	all other/thiol	10	4.68	0.0/+0.171[a]
$C(sp^3)$	all other/thiol	0.5	6.40	0.0/+0.171[a]
CH(aromatic)	thiophene	50.5	3.69	0.0
S	thiol	232	3.62	−0.377
S	sulfide	199	3.58	−0.300
S	disulfide	165	3.72	−0.177
S	thiophene	180	3.60	0.0
H	thiol	0	0	0.206

[a] For sites adjacent to sulfur in thiols. [b] For sites adjacent to sulfur in sulfides. [c] For sites adjacent to sulfur in disulfides.

for phase equilibria), this force field has grown to include alkenes and six-membered aromatic rings,[23] alcohols,[16] aldehydes, ethers, glycols, ketones,[20] carbonates,[24] amines, nitriles, and amides[25] as well as small molecules such as CO_2 and N_2.[26] In this work we present an extension of the TraPPE-UA (united-atom) force field to molecules containing thiol, sulfide, or disulfide functional groups and thiophene. Because of the transferable nature of the TraPPE-UA force field, only four new interaction sites were required. These are the Lennard−Jones ϵ and σ for sulfur, which are dependent on the bonding environment only. The required aliphatic C, CH, CH_2, and CH_3 and aromatic CH parameters were used without modification from previous development work for *n*-alkanes and benzene.[13,22,23]

This paper is organized as follows. The specific details of the functional form and the parametrization of the TraPPE-UA force field for thiols, sulfides, disulfides, and thiophene are given in the next section. Relevant details of the Monte Carlo simulations performed in this study are given in section 3. In section 4, the vapor−liquid coexistence curves and vapor pressures predicted by the TraPPE-UA force field are presented, followed by mixture phase diagrams for *n*-butane/ethanethiol and 1-propanethiol/*n*-hexane. The conclusions of this work can be found in section 5.

2. Models and Simulation Details

2.1. Force Fields. In the TraPPE-UA force field, hydrogens are combined with the carbons they are bonded to, forming a single interaction site, or "pseudoatom". Hydrogens bonded to heteroatoms, such as sulfur, are represented explicitly with a partial charge. A Lennard−Jones plus point charge functional form is used to represent interactions between nonbonded pseudoatoms

$$U(r_{ij}) = 4\epsilon_{ij}\left[\left(\frac{\sigma_{ij}}{r_{ij}}\right)^{12} - \left(\frac{\sigma_{ij}}{r_{ij}}\right)^{6}\right] + \frac{q_i q_j}{4\pi\epsilon_0 r_{ij}} \quad (1)$$

where r_{ij}, ϵ_{ij}, σ_{ij}, q_i, and q_j are the separation, LJ well depth, LJ size, and partial charges, respectively, for the pair of interaction sites i and j. As in previous implementations of the TraPPE-UA force field, nonbonded interactions are calculated for all intermolecular interactions as well as for intramolecular interactions of pseudoatoms separated by four or more bonds. The nonbonded parameters for the compounds studied in this work are listed in Table 1. We note that only C, CH, CH_2, and CH_3 pseudoatoms bonded to a polar sulfur atom have partial charges (but not those in thiophene). Interactions between unlike pseudoatoms are calculated with the Lorentz−Berthelot combining rules.[27,28]

$$\sigma_{ij} = (\sigma_{ii} + \sigma_{jj})/2 \quad (2)$$

$$\epsilon_{ij} = \sqrt{\epsilon_{ii}\epsilon_{jj}} \quad (3)$$

Pseudoatoms are connected by rigid bond lengths. A harmonic potential is used to control bond-angle bending

$$U_{\text{bend}} = \frac{k_\theta}{2}(\theta - \theta_0)^2 \quad (4)$$

where θ is the measured bond angle, θ_0 is the equilibrium bond angle, and k_θ is the force constant. Bending constants were derived by fitting eq 4 to the potential energy surfaces derived from ab initio calculations at the HF/6-31g+(d,p) level of theory. The bond lengths, bond angles, and bending constants used in this work are listed in Table 2. Torsional potentials used to restrict dihedral rotations around CH_x-CH_y, CH_x-S, and S−S bonds were taken from the OPLS-UA force field[29,30]

$$U_{\text{torsion}} = c_0 + c_1[1 + \cos(\phi)] + c_2[1 - \cos(2\phi)] + c_3[1 + \cos(3\phi)] \quad (5)$$

where ϕ and c_i are the dihedral angle and the ith coefficient, respectively. The necessary c_i coefficients are listed in Table 2. Required constants that were not found in the OPLS-UA parameter set were derived by fitting eq 5 to ab initio potential energy surfaces determined at the HF/6-31g+(d,p) level of theory and basis set.

2.2. Parametrization. In previous installments of the TraPPE-UA force field, partial charges have been taken directly from the OPLS-UA force field. In general, charges for the OPLS-UA force field were determined empirically, guided by a Mulliken analysis[31] of ab initio calculations at the HF/6-31g(d) level.[32] However, in the development of the OPLS-UA force field for sulfur compounds, the Mulliken analysis was found to be unreliable.[30] As a result, the OPLS-UA charges for sulfur compounds were developed to reproduce the energetics of various molecule complexes of sulfur compounds with water and Na^+. The OPLS-UA partial charges yield dipole moments that are significantly larger than experiment. For example, the dipole moment of the OPLS-UA H_2S model is 2.1 D, compared the experimental value of 1.0 D. Recent calculations have shown that the OPLS-UA charges for H_2S yield liquid-phase structures that display hydrogen bonding that is *not* seen in radial distribution functions extracted from neutron scattering.[33] In a recent work, Delhommelle et al. demonstrated that it was possible to generate reliable and unambiguous partial charges for sulfur compounds by fitting charges to the ab initio derived electrostatic potential (ESP).[21] In the case of H_2S, models derived from charges parametrized from ESP-type schemes were found to be in excellent agreement with radial distribution functions extracted from X-ray and neutron scattering experiments.[33,34]

In this work, the CHELPG (charges from electrostatic potentials using a grid based method) scheme was used to derive partial charges for the compounds of interest.[35,36] In this method, the molecular electrostatic potential (MEP) is calculated at a number of grid points spaced 3.0 pm apart, distributed regularly in a cube. The dimensions of the cube are chosen such that the molecule is located at the center with 28.0 pm headspace between the molecule and the end of the box in all three dimensions. All points falling inside the van der Waals radius of the molecule are discarded from the fitting procedure. Atomic charges are fit to reproduce the MEP after evaluating the MEP at all valid grid points. The only additional constraint in the

TABLE 2: TraPPE-UA Force Field Parameters for Bonded Interactions

vibration	bond length (Å)	bending	bond angle (deg)	k_θ/k_b (K)
S−H	1.34	∠ CH_x−S−H	96.0	33 830
CH_x−S (aliphatic)	1.82	∠ CH_y−CH_x−S	114.0	62 500
CH−S (aromatic)	1.71	∠ CH_x−CH_2−CH_y	114.0	62 500
CH_x−CH_y	1.54	∠ CH_y−S−CH_x	99.0	45 550
CH−CH (aromatic)	1.40	∠ CH_y−S−S	103.0	45 550
		∠ CH−CH−S (thiophene)	111.5	rigid
		∠ CH−S−CH (thiophene)	92.2	rigid
		∠ CH−CH−CH (thiophene)	112.4	rigid

torsion	c_0/k_b (K)	c_1/k_b (K)	c_2/k_b (K)	c_3/k_b (K)
CH_x−CH_2−S−H	52.88	−52.05	18.46	306.36
CH_y−CH_x−S−CH_x	0.0	367.6	−270.18	581.64
CH_x−S−S−CH_x	1763.9	398.0	−2181.6	505.25
CH_x−CH_2−CH−S	−251.06	428.73	−111.85	441.27
CH_x−CH_2−C−S	0.0	0.0	0.0	461.29
CH_3−CH−S−H	0.0	0.0	0.0	400.0

fitting procedure is that the sum of all atomic charges must equal the overall charge of the system. Calculations were performed at the HF/6-31+g(d,p) level of theory for methanethiol, dimethyl sulfide, dimethyl disulfide, and thiophene in vacuum with the Gaussian 03 program.[37] Ab initio calculations performed on ethanethiol utilizing an implicit solvent with a dielectric constant equal to that of the liquid phase showed only a minor (Δq = 0.06) increase in the magnitude of the partial charges compared to those performed under vacuum conditions. The choice of the Hartree−Fock theory and 6-31+g(d,p) basis set was based on our previous modeling efforts for H_2S, which showed that this combination of theory and basis set provided the best nonempirical estimate of partial charges when compared to MP2/aug-cc-pVQZ and MP2/6-31+g(d,p) calculations.[34] The same partial charges were used for all molecules in a particular homologous series. For example, the same charges were used for methane-, ethane-, pentane-, and octane-thiol and also for secondary and tertiary thiols as done previously for alcohols.[16]

The charge assignment for thiophene differs from those for the aliphatic sulfur-containing molecules. Because the CHELPG charges for thiophene are very small with a value of +0.023 e on the sulfur atom, a value of −0.034 e for the C2 and C5 pseudoatoms (pseudoatoms bonded to sulfur), and the remainder on the C3 and C4 united atoms, it was decided to neglect partial charges altogether.

Once the partial charges were determined, Lennard−Jones parameters for the sulfur atom in methanethiol, dimethyl sulfide, and dimethyl disulfide were fit to minimize the deviation between simulation and experiment with respect to saturated liquid densities and vapor pressures. In some cases it was not possible to reproduce both the vapor pressure and the saturated liquid density to high accuracy. In these cases, an emphasis was placed on reproduction of saturated liquid densities. The necessary parameters for the aliphatic C, CH, CH_2, CH_3, and aromatic CH pseudoatoms were taken from the TraPPE-UA force field for alkanes.[13,22,23]

3. Simulation Details

3.1. Grand Canonical Monte Carlo. Grand canonical histogram-reweighting Monte Carlo simulations[38,39] were used to determine the vapor−liquid coexistence curves and vapor pressures for thiols, sulfides, and disulfides as well as the binary mixtures ethanethiol/*n*-butane and 1-propanethiol/*n*-hexane. The insertion of molecules in the GCMC simulations were enhanced through multiple first bead insertions[40] and the application of the coupled-decoupled configurational-bias Monte Carlo method.[22,41] For binary mixture calculations, particle identity exchanges were used to enhance the sampling of composition space. The fractions of the various moves for each simulation were set to 15% particle displacements, 15% rotations, 10% coupled-decoupled configurational bias regrowths, and 60% insertions and deletions. Simulations were performed for system sizes of L = 25 Å for CH_3SH and CH_3CH_2SH, while box sizes of 30 and 35 Å were used for simulations of pentane- and octane- thiol, respectively. Simulations of all sulfides and disulfides were performed with a box size of L = 30 Å. Lennard−Jones interactions were truncated at L = 10 Å, and standard long-range corrections were applied.[43,44] An Ewald sum with tinfoil boundary conditions ($\kappa \times L = 5$ and $K_{max} = 5$) was used to calculate the long-range electrostatic interactions.[45,46] Simulations were equilibrated for 1 million Monte Carlo steps before run statistics were recorded, while production runs were 20 million MCS for liquid-phase simulations and 10 million MCS for calculations performed at vapor densities. Between five and nine total simulations were required to generate a complete phase diagram, where the number of simulations depended on system size and molecule type. In general, as system sizes increases, the range of thermodynamic state points covered by a given histogram is reduced. Over the course of each simulation, the number of molecules, N, and energy, E, (or N_1, N_2, E for mixtures) were stored in the form of a list, which was updated every 250 MCS. The necessary probability distributions were extracted from this list after the completion of the simulation.

3.2. Gibbs Ensemble Monte Carlo. Configurational-bias Monte Carlo simulations in the Gibbs ensemble[42] were carried out for thiophene. Like for the TraPPE-UA representation of other aromatic rings,[23] thiophene was treated as a rigid, planar ring. The simulations used a system size of 300 molecules with the total volume adjusted so that about 40−60 molecules were found on average in the vapor phase. Lennard−Jones interactions were truncated at L = 14 Å, and standard long-range corrections were applied.[43,44] The production periods consisted of 24 million MCS.

3.3. Isobaric−Isothermal Monte Carlo. Monte Carlo simulations in the isobaric−isothermal ensemble were used to determine the radial distribution functions for methanethiol. A system size of 500 molecules was used. Simulations were equilibrated for 25 million MCS, after which run statistics were recorded for an additional 25 million MCS. The ratio of moves was 1% volume changes, 14% configurational bias regrowths, 70% translations, and 15% molecule rotations. Lennard−Jones interactions were truncated at L = 10 Å, and standard long-range corrections were applied.[44,43] An Ewald sum with tinfoil

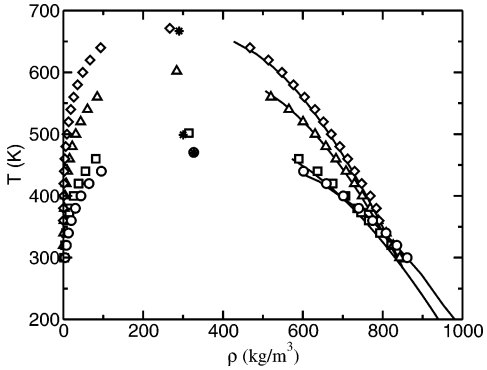

Figure 1. Vapor−liquid coexistence curves for methanethiol (circle), ethanethiol (square), pentanethiol (triangle), and octanethiol (Diamond). Solid lines depict the saturated liquid densities predicted by the Yaws correlation.[47] Stars denote experimental critical points.[5]

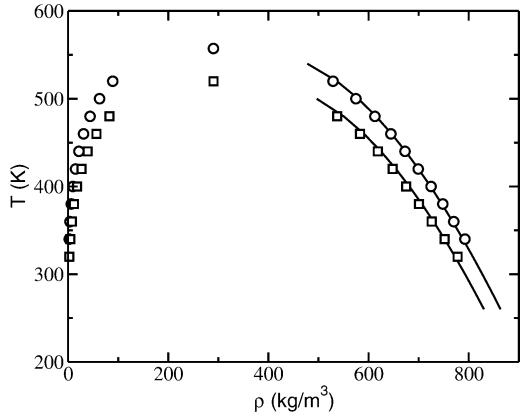

Figure 2. Vapor−liquid coexistence curves for 2-methyl-1-propanethiol (circle) and 2-methyl-2-propanethiol (square). Solid lines depict the saturated liquid densities predicted by the Yaws correlation.[47]

boundary conditions ($\kappa \times L = 5$ and $K_{max} = 5$) was used to calculate the long-range electrostatic interactions.[45,46]

4. Results and Discussion

4.1. Pure-Component Vapor−Liquid Equilibrium. *4.1.1. Thiols.* The pure-component saturated vapor and liquid densities predicted by the TraPPE-UA force field for linear and branched thiols are shown in Figures 1 and 2, respectively. Because of the lack of experimental data, a comparison is made to the correlation derived by Yaws[47] for saturated liquid densities. In contrast to the TraPPE-UA parametrization for alcohols, it was not necessary to alter the σ parameter for the α-C or α-CH pseudoatoms in the branched thiols. Although the large diameters of the C and CH pseudoatoms were found to negatively impact hydrogen bonding in alcohols,[16] thiols exhibit little, if any, hydrogen bonding[48] and the effects of such steric hindrances are minor for thiols. The reproduction of the saturated liquid densities is excellent for all of the thiols, demonstrating the transferability of the parameters developed for methanethiol to longer, as well as branched, thiols.

The vapor pressures for linear and branched thiols are shown in the form of Clausius−Clapeyron plots in Figures 3 and 4. The reproduction of vapor pressure for methanethiol is excellent, but deviations occur for longer thiols. This is due, in part, to the overestimation of vapor pressure built into the TraPPE *n*-alkane force field. Because the same parameters are used for the CH_2 and CH_3 pseudoatoms in this work, it is expected that as chain length increases, the deviation of the vapor pressure from experiment will also increase.

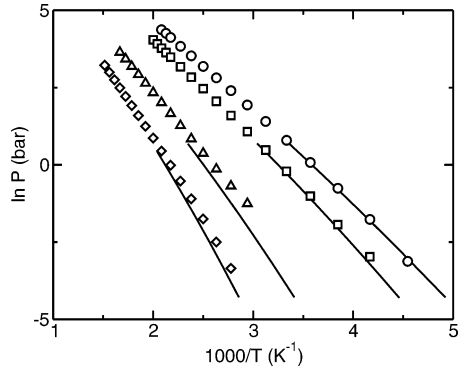

Figure 3. Clausius Clapeyron plot of the saturated vapor pressure vs inverse temperature as predicted by the TraPPE-UA force field for methanethiol (circle), ethanethiol (square), pentanethiol (triangle), and octanethiol (Diamond). The correlation of Yaws for the vapor pressure is shown as a solid line.[47]

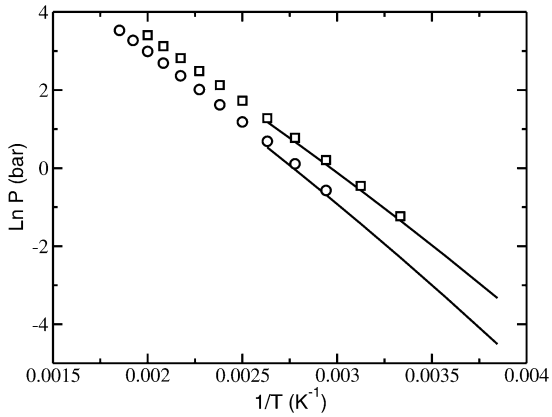

Figure 4. Clausius Clapeyron plot of the saturated vapor pressure vs inverse temperature as predicted by the TraPPE-UA force field for 2-methyl-1-propanethiol (circle) and 2-methyl-2-propanethiol (square). The correlation of Yaws for the vapor pressure is shown as a solid line.[47]

In Table 3, we compare the normal boiling point and critical properties predicted by the TraPPE-UA force field to experiment as well as the OPPE (optimized potentials for phase equilibria) force field developed recently.[21] Critical temperatures and densities were estimated by fitting the saturated liquid and vapor densities to the density scaling law for critical temperature[49]

$$\rho_{liq} - \rho_{vap} = B(T_c - T)^{\beta} \tag{6}$$

and the law of rectilinear diameters[50]

$$\frac{\rho_{liq} + \rho_{vap}}{2} = \rho_c + A(T - T_c) \tag{7}$$

where $\beta = 0.325$ is the critical exponent for Ising-type fluids in three dimensions[51] and A and B are constants fit to simulation data. For each of the thiols, the TraPPE-UA predicts critical temperatures that are slightly (<1%) higher than those of the experiment, but generally within the uncertainty of the experimental measurement. The accuracy of ρ_c varies from <0.6% deviation for methanethiol to 8.0% for 1-octanethiol. However, the uncertainty in the experimental data is significant. For example, there is approximately a 7% uncertainty in the reported critical density for octanethiol, which is nearly as large as the deviation of simulation from experiment. The OPPE force field yields T_c and ρ_c with an accuracy similar to that of TraPPE-UA. The critical pressure was determined by extrapolating the

TABLE 3: Pure-Component Properties for Thiols, Sulfides, and Disulfides

molecule		T_c (K)	ρ_c (kg/m^3)	P_c (bar)	T_b (K)
methanethiol	TraPPE-UA	475	326	75.5	278.1
	experiment[5,55]	470 ± 2	327 ± 10	72.3 ± 2.0	279.1
	OPPE[21]	477	320		
ethanethiol	TraPPE-UA	502	314	59.6	306.7
	experiment[5,55]	499 ± 2	300 ± 10	54.9 ± 2.0	308.2
	OPPE[21]	496	291		
2-methyl-1-propanethiol	TraPPE-UA	557	290	42.9	356.3
	experiment				
2-methyl-2-propanethiol	TraPPE-UA	520	290	39.8	334.4
	experiment				
2-butanethiol	TraPPE-UA	557	293	44.6	353.7
	experiment				
pentanethiol	TraPPE-UA	602	284	36.0	380.3
	experiment[55]				399.8
octanethiol	TraPPE-UA	671	267	33.9	466.4
	experiment[5,55]	667 ± 7	290 ± 20		472.3
dimethyl sulfide	TraPPE-UA	504	313	59.3	302.8
	experiment[5,55]	503 ± 1	305 ± 5	55.3 ± 1.0	310.5
	OPPE[21]	511	312		
diethyl sulfide	TraPPE-UA	562	289	42.8	357.9
	experiment[5,55]	557.8 ± 0.2	284 ± 5	39.0 ± 0.2	365.3
	OPPE[21]	565	284		
ethylmethyl sulfide	TraPPE-UA	536	298	50.5	333.0
	experiment[5,55]	533 ± 1		42.5 ± 4.0	339.9
	OPPE[21]	537	285		
dimethyl disulfide	TraPPE-UA	606	362	53.4	375.8
	experiment[5]	615 ± 10			382.9
diethyl disulfide	TraPPE-UA	658	321	42.3	429.6
	experiment[5]	642 ± 10			427.2
thiophene	TraPPE-UA	605	375	70.6	357.4
	experiment[5,55]	580 ± 1	385	57.0	357.3

vapor pressure curve to the critical temperature. The TraPPE-UA force field was found to overpredict the critical pressures of methane- and ethane-thiol by 4% and 9%, respectively. Experimental critical pressures for other thiols were not available for comparison.

The normal boiling points were determined through interpolation of simulation data on the Clausius−Clapeyron plot. As expected from the excellent reproduction of the vapor pressure, the normal boiling point predicted for methanethiol is in excellent agreement with experiment. As in the case of the critical density, the experimental data set appears to have minor inconsistencies. The T_b predicted by the TraPPE-UA force field for pentanethiol is 5% lower than experiment; however, the deviation in the normal boiling point for octanethiol is only 1.2%. This is despite the fact that one would expect the predictions of the vapor pressure to become less accurate as chain length increases because of the inherent limitations of the original TraPPE-UA parameters for CH_2 and CH_3 pseudoatoms.

Simulations in the isobaric−isothermal ensemble at 279 K and 1 bar (the normal boiling point) were performed to determine the liquid-phase radial distribution functions for methanethiol. For comparison, the RDFs predicted by the OPLS-UA[30] and OPPE[33] force fields are also shown. The TraPPE-UA and OPPE force fields yield similar RDFs, which suggest a featureless fluid structure. The OPLS-UA force field shows a peak at approximately 2.2 Å, suggesting the presence of hydrogen bonding. It should be noted that the dipole moment of methanethiol as given by the OPLS-UA force field is overpredicted by approximately 50%. Unfortunately, no experimental pair correlation data exist to make a definitive conclusion as to which force field provides the best prediction

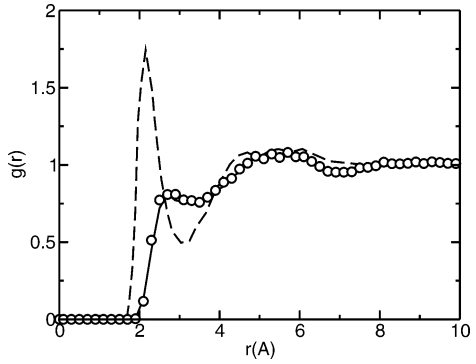

Figure 5. H−S radial distribution function for liquid methanethiol at 279 K and 1 bar. Results are presented as: TraPPE-UA (circle), OPPE (solid line),[21] and OPLS-UA (dashed line).

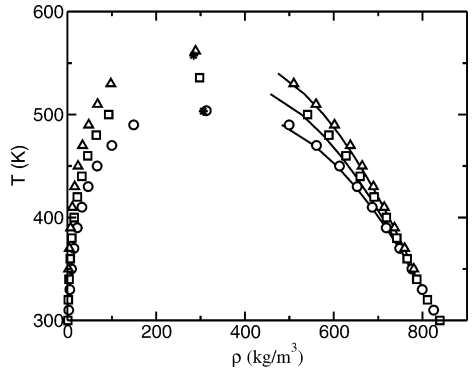

Figure 6. Vapor−liquid coexistence curves for dimethyl sulfide (circle), diethyl sulfide (triangle), and ethylmethyl sulfide (Square). The predictions of the Yaws correlation for saturated liquid densities are plotted as a solid line.[47] Stars denote experimental critical points.[5]

of the liquid-phase structure. Recent ab initio calculations, however, support the hypothesis of a featureless liquid structure. Calculations performed at the HF/6-31G** level failed to show lengthening of the S−H bond in clusters of 2, 3, and 4 methanethiol molecules.[48] Such lengthening is an indication of hydrogen-bond cooperative effects and is seen clearly in ab inito calculations performed on clusters of primary alcohols.[48] Furthermore, H_2S has been shown by neutron scattering not to exhibit any significant hydrogen bonding in the liquid phase. Therefore, it is more plausible that limited, if any, hydrogen bonding will be present in liquid thiols.

4.1.2. Sulfides. Because of the different bonding environment, it was not possible to use the same Lennard−Jones parameters for the sulfur atom in sulfides as in thiols. Parameters for sulfides were determined by tuning the σ and ϵ for the sulfur atom to minimize to deviation of simulation from experiment with respect to the saturated liquid densities for dimethyl sulfide. In Figure 6, the vapor−liquid coexistence curves for dimethyl sulfide, diethyl sulfide, and ethylmethyl sulfide, as predicted by the TraPPE-UA force field, are presented. As in the case of thiols, experimental VLE data are very limited for disulfides. For this reason, the simulation data are shown in comparison to the Yaws correlation for saturated liquid density.[47] Overall, there is an excellent reproduction of the saturated liquid density by the TraPPE-UA force field. Vapor pressures are presented in the form of a Clausius−Clapeyron plot in Figure 7 and show that the TraPPE-UA force field slightly overpredicts the vapor pressure of sulfides over the entire coexistence curve. The critical properties and normal boiling points were calculated with the same methodology as described above for thiols. The TraPPE-UA force field predicts critical temperatures that are approximately 0.5% higher than experiment, whereas slightly

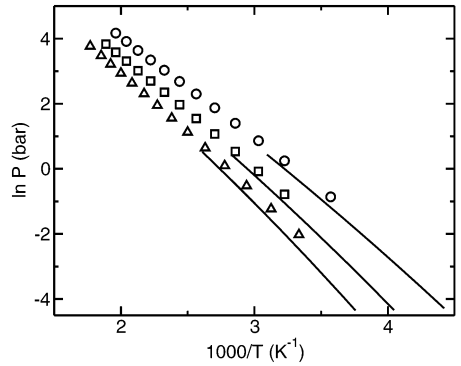

Figure 7. Clausius−Clapeyron plot for dimethyl sulfide (circle), diethyl sulfide (triangle), and ethylmethyl sulfide (Square). The predictions of the Yaws correlation for vapor pressure are presented as solid lines.[47]

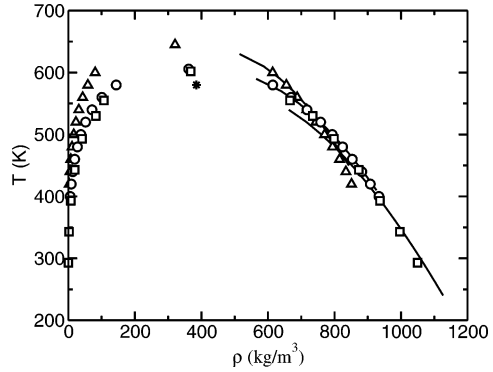

Figure 8. Vapor−liquid coexistence curves for dimethyl disulfide (circle), diethyl disulfide (triangle), and thiophene (square). Solid line denotes the predictions of the Yaws correlation for saturated liquid density.[47] Star denotes experimental critical point for thiophene.[5]

larger deviations are found in ρ_c. The normal boiling points are well reproduced, with the maximum deviation being a 2.5% underprediction for dimethyl sulfide.

4.1.3. Disulfides. A third set of Lennard−Jones parameters were fit for sulfur atoms that participate simultaneously in CH_x−S and S−S bonds. Simulations of dimethyl disulfide were used to tune parameters such that the difference between simulation and experiment in the saturated liquid density was minimized. The results of these calculations for the vapor−liquid coexistence curve are shown in Figure 8. The transferability of the force field is assessed through calculations of diethyl disulfide. At lower temperatures, the TraPPE-UA force field was found to underpredict the saturated liquid density of diethyl sulfide by approximately 2%. The vapor pressures predicted by the TraPPE-UA force field are presented in Figure 9 and are in good agreement with experiment. The critical properties, T_c, ρ_c, p_c, and normal boiling points predicted by the TraPPE-UA force field, listed in Table 3, are all within 2% of experiment.

4.1.4. Thiophene. A fourth sulfur parameter was required for thiophene because the bonding environment to the neighboring aromatic CH groups is different than that to aliphatic groups in sulfides. However, as can be seen from the Lennard−Jones parameters listed in Table 1, the parameters for sulfur in thiophene fall between those for sulfides and disulfides. The experimental vapor pressure,[53] the heat of vaporization at the boiling point,[54] and the liquid density[55] were used as targets for the fit of the sulfur site in thiophene. A comparison with experiment for thiophene's vapor−liquid coexistence and saturated vapor pressure curves is shown in Figures 8 and 9. The target data are all well reproduced by the TraPPE-UA

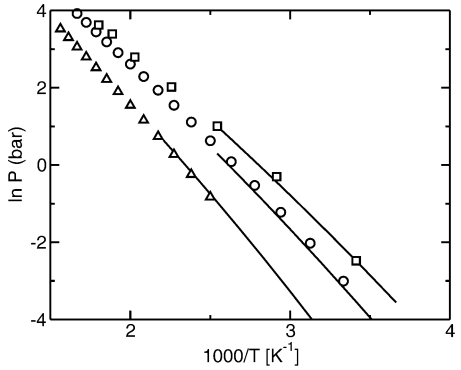

Figure 9. Clausius−Clapeyron plots for dimethyl disulfide (circle), diethyl disulfide (triangle), and thiophene (square). The vapor pressures predicted by the Yaws correlation (disulfides) or experiment (thiophene) are shown as solid lines.[47,53]

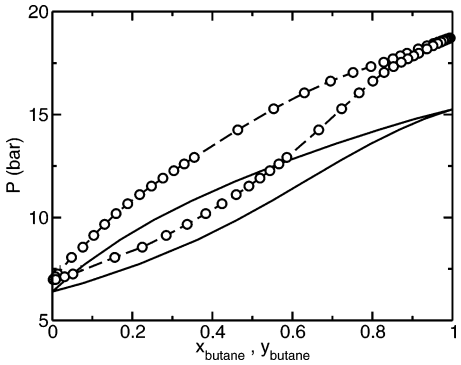

Figure 10. Pressure−composition diagram for *n*-butane(1)+ethanethiol-(2) at 373.15 K. Circles represent the predictions of the TraPPE-UA force field, and solid lines are used to denote experimental data.[3] The dashed line is provided as a guide to the eye. Statistical uncertainties in the coexistence pressures are approximately the size of the symbols.

thiophene model, but it appears that the critical temperature is overestimated by about 4% and the critical density is correspondingly underestimated.

4.2. Binary Mixture Phase Behavior. Knowledge of the phase behavior of binary mixtures of sulfur-containing compounds and hydrocarbons is important for the development of separation processes related to the production of natural gas as well as the refinement of motor vehicle fuels. Despite the importance of these data, limited binary VLE data are available in the literature. Two systems for which binary VLE data exist are *n*-butane(1)+ethanethiol(2)[3] and 1-propanethiol(1)+*n*-hexane(2).[1] In Figure 10, the predictions of the TraPPE-UA force field for the pressure composition behavior of *n*-butane(1)-ethanethiol(2) at 373.15 K is presented. Good agreement between simulation and experiment is achieved, with the major deviation arising from the overprediction of the pure-component vapor pressure of *n*-butane. The width of the predicted *Pxy* curve is slightly wider than experiment, suggesting a slight underprediction of unlike-molecule interactions. The temperature−composition behavior for the 1-propanethiol(1)+*n*-hexane(2) system was determined at 1.01 bar and is compared to experimental data in Figure 11. Qualitatively, there is an excellent reproduction of the *Txy* behavior for this mixture. However, because the vapor pressures of the pure components are slightly overpredicted, there is a corresponding underprediction of the normal boiling points, which shifts the entire coexistence curve to lower temperatures. Despite these shifts of the coexistence curve, the prediction of separation factors $k_i = y_i/x_i$ is quite good. In Figure 12, a plot of vapor phase mole fraction versus liquid phase mole fraction of thiol is presented

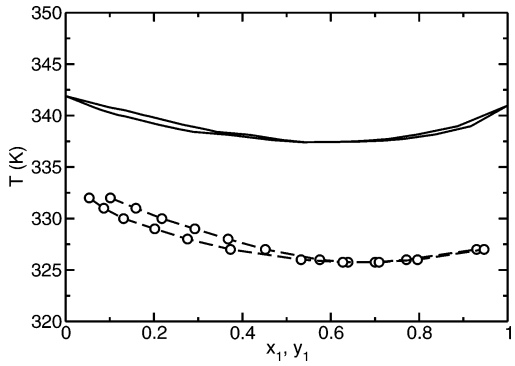

Figure 11. Temperature−composition diagram for 1-propanethiol-(1)+*n*-hexane(2) at 1.01325 bar. Circles represent the predictions of the TraPPE-UA force field, and solid lines are used to denote experimental data.[1] The dashed line is provided as a guide to the eye. Statistical uncertainties in the coexistence temperatures are approximately twice the size of the symbols.

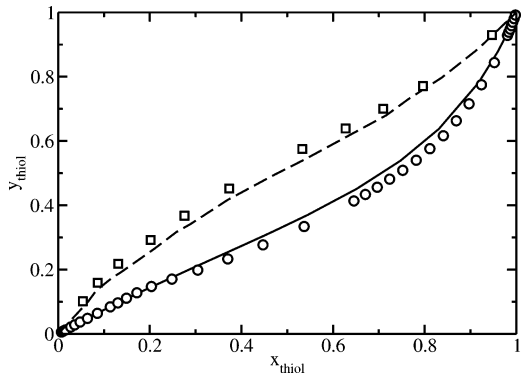

Figure 12. Plot of vapor phase mole fraction of thiol vs liquid-phase mole fraction of thiol for ethanethiol+*n*-butane (circles) and 1-propanethiol+*n*-hexane (squares). Solid and dashed lines represent experimental data for ethanethiol+*n*-butane[3] and 1-propanethiol+*n*-hexane,[1] respectively.

for both mixtures. Simulations of the TraPPE-UA force field exhibit only minor deviations from experiment. This demonstrates that the TraPPE-UA force field provides a good representation of interspecies interactions in alkane−thiol mixtures. Unlike other mixtures of polar and nonpolar components, such as alkanol-alkane,[16,56] thiols do not self-associate to any significant extent. Therefore, a detailed analysis of the liquid-phase structure of either mixture was not performed.

5. Conclusions

The TraPPE-UA force field was extended to thiols, sulfides, disulfides, and thiophene through the introduction of four new interaction sites for sulfur. Excellent agreement with experimental saturated liquid densities and critical temperatures was achieved, with unsigned deviations from experiment of <1% in most cases. Only the calculations of diethyl disulfide show any significant deviation from experiment with respect to saturated liquid densities. The normal boiling points for many of the molecules of interest were predicted within 2.5% of experiment. The binary vapor−liquid equilibrium data, as predicted by the TraPPE-UA force field, for the *n*-butane-(1)+ethanethiol(2) and 1-propanethiol(1)+*n*-hexane(2) systems show good agreement with experiment for the separation factors; however, the overprediction of the pure-component vapor pressures results in somewhat shifted coexistence curves.

Acknowledgment. Financial support from the National Science Foundation (CTS-0522005, DGE-9987598, and CTS-0138393) and a Minnesota Supercomputing Institute Research Scholarship (J.J.P) are gratefully acknowledged. Part of the computer resources used in this work were provided by the Minnesota Supercomputing Institute.

Supporting Information Available: The numerical data for the saturated liquid and vapor densities and vapor pressures for the neat systems are listed in Tables 1−8. The numerical data for the vapor- and liquid-phase compositions for the two binary systems are listed in Tables 9 and 10. This material is available free of charge via the Internet at http://pubs.acs.org.

References and Notes

(1) Denyer, R. L.; Fidler, F. A.; Lowry, R. A. *Ind. Eng. Chem.* **1949**, *41*, 2727.
(2) Wolff, H.; Szydlowski, J.; Dill-Staffenberger, L. *J. Chem. Thermodyn.* **1980**, *12*, 641.
(3) Giles, N. F.; Wilson, G. M. *J. Chem. Eng. Data* **2000**, *45*, 146.
(4) Kilner, J.; McBain, S. E.; Roffey, M. G. *J. Chem. Thermodyn.* **1990**, *22*, 203.
(5) Tsonopoulous, C.; Ambrose, D. J. *Chem. Eng. Data.* **2001**, *46*, 480.
(6) Twu, C. H.; Tassone, V.; Sim, W. D. *Chem. Eng. Prog.* **2004**, *100*, 39.
(7) MacKerell, A. D., Jr.; Wirkiewicz-Kuczera, J.; Karplus, M. *J. Am. Chem. Soc.* **1995**, *117*, 11946.
(8) MacKerell, A. D., Jr.; Basford, D.; Bellot, M.; Dunbrack, J.; Evanseck, J. D.; Field, M. J.; Fischer, S.; Gao, J.; Guo, H.; Ha, S.; Joseph-McCarty, D.; Kuchnin, L.; Kuczera, K.; Lau, F. T. W.; Mattos, C.; Michnick, S.; Ngo, T.; Nguyen, D. T.; Prodhom, B.; Reiher, W. E.; Roux, B.; Schlenkrich, M.; Smith, J. C.; Stote, R.; Strauh, J.; Watannabe, M.; Wirkiewicz-Kuczera, J.; Yin, D.; Karplus, M. *J. Phys. Chem. B.* **1998**, *102* 3586.
(9) Cornell, W. D.; Cieplak, P.; Bayly, C. I.; Gould, I. R.; Merz, K. M., Jr.; Ferguson, D. M.; Spellmeyer, D. C.; Fox, T.; Caldwell, J. W.; Kollman, P. A. *J. Am. Chem. Soc.* **1995**, *117*, 5179.
(10) Halgren, T. A. *J. Comput. Chem.* **1996**, *17*, 490.
(11) Jorgensen, W. L.; Maxwell, D. S.; Tirado-Rives, J. *J. Am. Chem. Soc.* **1996**, *118*, 11225.
(12) Errington, J. R.; Panagiotopoulos, A. Z. *J. Phys. Chem. B* **1999**, *103*, 6314.
(13) Martin, M. G.; Siepmann, J. I. *J. Chem. Phys. B* **1998**, *102*, 2569.
(14) Nath, S. K.; Escobedo, F. A.; de Pablo, J. J. *J. Chem. Phys.* **1998**, *108*, 9905.
(15) Ungerer, P.; Beauvais, C.; Delhommelle, J.; Boutin, A.; Rousseau, B.; Fuchs, A. H. *J. Chem. Phys.* **2000**, *112*, 5499.
(16) Chen, B.; Potoff, J. J.; Siepmann, J. I. *J. Chem. Phys. B* **2001**, *105*, 3093.
(17) Khare, R.; Sum, A. K.; Nath, S. K.; de Pablo, J. J. *J. Phys. Chem. B* **2004**, *108*, 10071.
(18) Kamath, G.; Cao, F.; Potoff, J. J. *J. Phys. Chem. B* **2004**, *108*.
(19) Kranias, S.; Pattou, D.; Levy, B.; Boutin, A. *Phys. Chem. Chem. Phys.* **2003**, *5*, 4175.
(20) Stubbs, J. M.; Potoff, J. J.; Siepmann, J. I. *J. Phys. Chem. B* **2004**, *108*, 17596.
(21) Delhommelle, J.; Tschirwitz, C.; Granucci, G.; Millie, P.; Pattou, D.; Fuchs, A. H. *J. Phys. Chem. B* **2000**, *104*, 4745.
(22) Martin, M. G.; Siepmann, J. I. *J. Phys. Chem. B* **1999**, *103*, 4508.
(23) Wick, C. D.; Martin, M. G.; Siepmann, J. I. *J. Phys. Chem. B* **2000**, *104*, 8008.
(24) Wick, C. D.; Siepmann, J. I.; Theodorou, D. N. *J. Am. Chem. Soc.* **2005**, *127*, 12338.
(25) Wick, C. D.; Stubbs, J. M.; Rai, N.; Siepmann, J. I. *J. Phys. Chem. B* **2005**, *109*, 18974.
(26) Potoff, J. J.; Siepmann, J. I. *AIChE J.* **2001**, *47*, 1676.
(27) Lorentz, H. A. *Ann. Phys.* **1881**, *12*, 127.
(28) Berthelot, D. C. *R. Hebd. Seanc. Acad. Sci., Paris* **1898**, *126*, 1703.
(29) Jorgensen, W. L.; Madura, J. D.; Swenson, C. J. *J. Am. Chem. Soc.* **1984**, *106*, 6638.
(30) Jorgensen, W. L. *J. Phys. Chem.* **1986**, *90*, 6379.
(31) Mulliken, R. S. *J. Chem. Phys.* **1955**, *23*, 1833.
(32) Jorgensen, W. L. *J. Phys. Chem.* **1986**, *90*, 1276.
(33) Delhommelle, J.; Millie, P.; Fuchs, A. H. *Mol. Phys.* **2000**, *98*, 1895.
(34) Kamath, G.; Lubna, N.; Potoff, J. J. *J. Chem. Phys.* **2005**, *123*, 124505.
(35) Breneman, C. M.; Wilberg, K. B. *J. Comput. Chem.* **1990**, *11*, 361.
(36) Cox, S. R.; Williams, D. E. *J. Comput. Chem.* **1981**, *2*, 304.
(37) Frisch, M. J.; Trucks, G. W.; Schlegel, H. B.; Scuseria, G. E.; Robb, M. A.; Cheeseman, J. R.; Montgomery, J. A., Jr.; Vreven, T.; Kudin, K.

N.; Burant, J. C.; Millam, J. M.; Iyengar, S. S.; Tomasi, J.; Barone, V.; Mennucci, B.; Cossi, M.; Scalmani, G.; Rega, N.; Petersson, G. A.; Nakatsuji, H.; Hada, M.; Ehara, M.; Toyota, K.; Fukuda, R.; Hasegawa, J.; Ishida, M.; Nakajima, T.; Honda, Y.; Kitao, O.; Nakai, H.; Klene, M.; Li, X.; Knox, J. E.; Hratchian, H. P.; Cross, J. B.; Bakken, V.; Adamo, C.; Jaramillo, J.; Gomperts, R.; Stratmann, R. E.; Yazyev, O.; Austin, A. J.; Cammi, R.; Pomelli, C.; Ochterski, J. W.; Ayala, P. Y.; Morokuma, K.; Voth, G. A.; Salvador, P.; Dannenberg, J. J.; Zakrzewski, V. G.; Dapprich, S.; Daniels, A. D.; Strain, M. C.; Farkas, O.; Malick, D. K.; Rabuck, A. D.; Raghavachari, K.; Foresman, J. B.; Ortiz, J. V.; Cui, Q.; Baboul, A. G.; Clifford, S.; Cioslowski, J.; Stefanov, B. B.; Liu, G.; Liashenko, A.; Piskorz, P.; Komaromi, I.; Martin, R. L.; Fox, D. J.; Keith, T.; Al-Laham, M. A.; Peng, C. Y.; Nanayakkara, A.; Challacombe, M.; Gill, P. M. W.; Johnson, B.; Chen, W.; Wong, M. W.; Gonzalez, C.; Pople, J. A. *Gaussian 03*, revision C.02; Gaussian, Inc.: Wallingford, CT, 2004.

(38) Potoff, J. J.; Panagiotopoulos, A. Z. *J. Chem. Phys.* **1998**, *109*, 10914.

(39) Potoff, J. J.; Errington, J. R.; Panagiotopoulos, A. Z. *Mol. Phys.* **1999**, *97*, 1073.

(40) Esselink, K.; Loyens, L. D. J. C.; Smit, B. *Phys. Rev. E* **1995**, *51*, 1560.

(41) Siepmann, J. I.; Frenkel, D. *Mol. Phys.* **1992**, *75*, 59.

(42) Panagiotopoulos, A. Z. *Mol. Phys.* **1987**, *61*, 813.

(43) McDonald, I. R. *Mol. Phys.* **1972**, *23*, 41.

(44) Wood, W. W. *J. Chem. Phys.* **1968**, *48*, 415.

(45) Ewald, P. P. *Ann. Phys.* **1921**, *64*, 253.

(46) Allen, M. P.; Tildesley, D. J. *Computer Simulation of Liquids*, 1st ed.; Oxford University Press: New York, 1987.

(47) Yaws, C. L. *Thermodynamic and Physical Property Data*; Gulf Publishing Company: Houston, TX, 1992.

(48) Sum, A. K.; Sandler, S. I. *J. Phys. Chem. A* **2000**, *104*, 1121.

(49) Rowlinson, J. S.; Widom, B. *Molecular Theory of Capillarity*, Clarendon Press: Oxford, 1982.

(50) Rowlinson, J. S.; Swinton, F. L. *Liquids and Liquid Mixtures*, 3rd ed.; Butterworth: London, 1982.

(51) Privman, V. In *Encyclopedia of Applied Physics*; Trigg, G. L., Ed.; Wiley-VCH: Berlin, 1998; Vol. 23, p 41.

(52) Daubert, T. E.; Danner, R. P. *Physical and Thermodynamic Properties of Pure Chemicals*; Taylor and Francis Inc., 1994.

(53) Waddington, G.; Knowlton, J. W.; Scott, D. W.; Oliver, G. D.; Todd, S. S.; Hubbard, W. N.; Smith, J. C.; Huffman, H. M. *J. Am. Chem. Soc.* **1949**, *71*, 797.

(54) Major, V.; Svoboda, V. *Enthalpies of Vaporization of Organic Compounds: A Critical Review and Data Compilation*; Blackwell Scientific Publications: Oxford, 1985; p 300.

(55) Lide, D. A. *CRC Handbook of Chemistry and Physics*; CRC Press: Boca Raton, FL, 1991.

(56) Stubbs, J. M.; Siepmann, J. I. *J. Phys. Chem. B* **2002**, *106*, 3968.